

Animated-beam measurement of the photodetachment cross section of H^-

Matthieu Génévriez* and Xavier Urbain

Institute of Condensed Matter and Nanosciences, Université catholique de Louvain, Louvain-la-Neuve B-1348, Belgium

(Received 1 October 2014; revised manuscript received 3 December 2014; published 9 March 2015)

The photodetachment cross section of H^- was measured using the animated-crossed-beam technique in the 700- to 1064-nm range. The laser beam was repeatedly swept across the ion beam by tilting a fused silica plate in order to eliminate the need for beam profile measurements. After integration of the signal, the cross section was expressed in terms of easily measurable quantities, e.g., the laser power and the ion beam current. The present results are in excellent agreement with previous experiments and compelling theoretical works.

DOI: [10.1103/PhysRevA.91.033403](https://doi.org/10.1103/PhysRevA.91.033403)

PACS number(s): 32.80.Gc, 37.20.+j

I. INTRODUCTION

The negative hydrogen ion H^- is the simplest of the quantum-mechanical three-body systems found in the study of atoms and ions. Its prototypical character has attracted numerous studies since the early days of quantum mechanics [1], further motivated by its abundance in the planetary and stellar atmospheres and its wide use in accelerators. Of particular interest is its photodetachment, where electron correlations in that weakly bound system play an important role and yield a behavior differing from that of neutral atoms.

Since the early studies of, e.g., Bates and Massey [2] and Chandrasekar [3], theory has made significant progresses. Over the years, a number of calculations of the photodetachment cross section have been performed reaching an overall good agreement, e.g., $3.5\text{--}3.6 \times 10^{-21} \text{ m}^2$ at 1064 nm [4–13], except for a few studies [14–16].

On the experimental side, however, fewer studies have been performed, due to the challenges such an experiment raises. The absolute integrated cross section was first measured by Branscomb and Smith [17] in the mid-1950s, shortly followed by the measurement of the relative cross section by Smith and Burch [18]. Popp and Kruse [19] later performed an absolute measurement with a low current hydrogen arc. The first laser studies arose with the need to diagnose controlled fusion plasmas, and confirmed the order of magnitude of the cross section [20,21]. Recently, Vandevraye *et al.* [22] carried out a new measurement at the Nd:YAG laser wavelength, 1064 nm. Their result, $4.5(6) \times 10^{-21} \text{ m}^2$, lies 1.5σ above the value of $3.5\text{--}3.6 \times 10^{-21} \text{ m}^2$ obtained by most theoretical studies. This possible discrepancy calls for further investigation to be carried out, as this cross section is a commonly used benchmark for atomic theories and numerical methods [23].

The present article describes an experimental measurement of the photodetachment cross section of H^- performed in our laboratory. The method implemented significantly differs from the saturation techniques used by Vandevraye *et al.* [22]. We adopted, in the linear regime of photodetachment, the animated-crossed-beam technique originally developed for electron-ion collisions by Brouillard and Defrance [24]. Assumptions on the shape of both laser and ion beams are not required, and the method is therefore expected to be more robust and reliable.

II. EXPERIMENT

The first stage of the experimental setup, sketched in Fig. 1, comprises a duoplasmatron source providing a 4-keV beam of H^- anions. After mass selection by a permanent magnet, a set of planar deflectors brings the beam to the interaction region, pumped to high vacuum (3×10^{-8} mbar). Two diaphragms, located on either side of the ion-laser interaction region, define the beam direction. These two diaphragms have further been carefully aligned with the apertures of the quadrupolar deflector and the channel electron multiplier (CEM) cone so the beam direction and the neutrals detection axis overlap.

The 1-mm H^- beam is illuminated perpendicularly by the light of a cw Ti:sapphire laser (3900S, Spectra Physics) pumped by an Ar^+ laser (Innova 400, Coherent), the latter delivering a maximum output power of 21 W in multiline operation. The Ti:sapphire laser operates at the TEM₀₀ mode and covers the 700- to 1000-nm wavelength range with an output power of more than 3 W at the center of the range. This range is further extended to 1064 nm by means of a cw diode pumped solid-state laser (DPSS-1064-H3000, Eksma Optics). The light is brought to the vacuum chamber by a set of mirrors and focused by an $f = 40$ cm lens onto the anion beam. A 10-mm-thick fused silica plate mounted on a rotating stage is placed just after the lens. By varying the angle of the plate, the angle of incidence of the laser beam can be varied and its vertical position after the plate can be modified at will, thus “animating” the beam (see Fig. 2).

On the other side of the vacuum chamber, the light is collected by a powermeter (S310C, Thorlabs) measuring the laser power with a 3% accuracy. Powers ranging from 0.5 to 2 W are reached in the interaction region throughout the wavelength range covered. A measurement of the laser power before and after the vacuum chamber showed no difference; hence the loss of photon flux due to the exit window of the chamber is contained within the accuracy of the powermeter. This confirms the manufacturer specifications, which give a reflectance of the coated window lower than 0.5% and an absorbance of the order of 0.1% (N-BK7).

After the second aperture, the ion beam enters the detection region. It first passes through a quadrupolar deflector, where negative ions are deflected on one side and collected in a Faraday cup connected to the input of a calibrated electrometer (614, Keithley). The neutral hydrogen atoms fly straight through the quadrupole and are detected about 30 cm downstream by a CEM (KBL 25 RS, Dr. Sijtsma Optotechnik).

*matthieu.genevriez@uclouvain.be

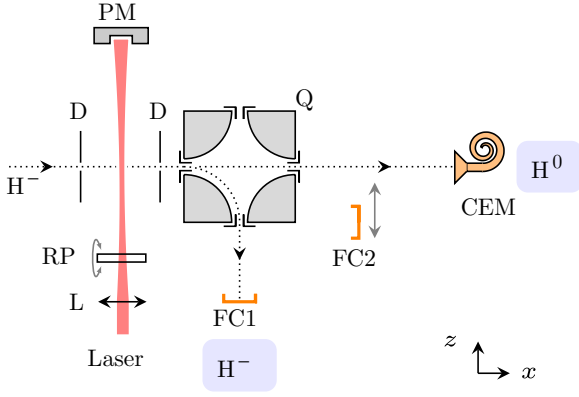


FIG. 1. (Color online) Experimental setup. D: diaphragm; FC: Faraday cup; Q: quadrupolar deflector; CEM: channel electron multiplier; L: lens; RP: rotating fused silica plate; PM: powermeter. The laser beam propagates along the z direction and its polarization is along the y axis.

Two parameters affect the detection of neutrals by the CEM: the detection efficiency η and the value of the counting rate N . The efficiency is estimated to be 0.98 ± 0.02 according to Naji *et al.* [25], who measured the efficiency of the exact same detector model. Furthermore, test measurements for a 6-keV beam showed no significant increase of the detection efficiency, suggesting that η has reached the asymptotic regime of efficiency versus particle energy, as expected from the CEM specifications. When too high ($\gtrsim 50$ kHz), the second parameter, the counting rate N , causes a non-negligible dead time and degrades the pulse height distribution. The main contribution to N comes from the collisional detachment with the residual gas occurring between the first diaphragm and the quadrupole. The ion beam intensity was therefore reduced to ~ 50 pA in order to maintain the counting rate below its maximum threshold. Typical values of 25 kHz are reached in operation.

When the quadrupolar deflector is switched off, a movable Faraday cup (FC2) can be used to collect the negative ions in a straight line aligned with the CEM entrance. The measured current, compared to the current measured in FC1 when the quadrupole is on, gives an accurate estimation of the alignment between the beam and detection axes. When the agreement between the two currents measured is reached, the axes overlap and we therefore ensure that no photodetached hydrogen atom misses the detector, i.e., that the normalization of the counting rate to the H^- current is consistent. After fine alignment, an agreement better than 1% was obtained between the two currents, which we take as the uncertainty on the H^- current value. A leakage current was observed in the Faraday cup FC1,

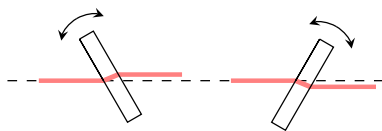


FIG. 2. (Color online) Laser beam passing through a glass plate. Refraction within the plate yields an output beam displaced along the vertical axis.

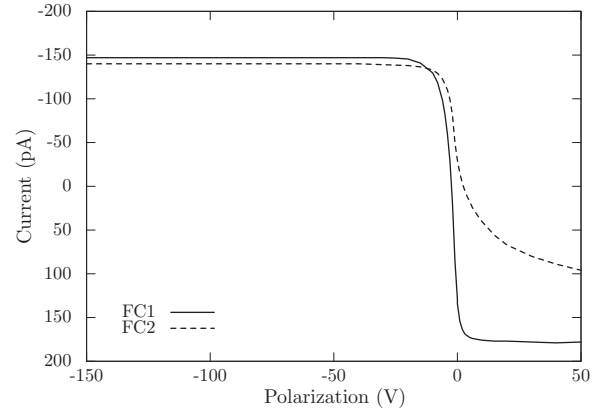


FIG. 3. Current (pA) measured by the Faraday cups FC1 and FC2 with respect to the polarization voltage (V) applied to the guard electrode of the cup. A polarization voltage of -100 V is applied to each cup throughout the experiment. The offset at negative voltages is the leakage current on FC1.

due to the neighboring high voltages of the quadrupole. The cup current was therefore calibrated accordingly, prior to each measurement.

Each Faraday cup is equipped with a guard electrode polarized at -100 V. We checked the behavior of the measured current as a function of the polarization voltage, as shown in Fig. 3. For sufficiently high negative voltages, typically below -50 V, a plateau is reached indicating that all secondary electrons emitted by the ion-surface collisions are confined within the cup, and therefore that the current measured faithfully reproduces the incoming ion beam current. The remaining difference between the currents measured by the two cups is solely the leakage current on FC1 discussed above. Furthermore, the radius of the ion beam is one third of the cup radius, hence excluding edge effects.

The rotating stage and powermeter are servocontrolled by an external computer. A data acquisition system (DAQ) monitors the Faraday cup current, given by the analog output of the electrometer and the CEM counting rate. All the variables required to obtain the cross section can thus be measured and stored in the computer. The experiment therefore consists in moving the rotating stage to a given angle and sequentially recording the laser power, neutrals count rate, and negative ion current.

We detailed above the experimental setup, yet did not explicitly discuss the important role played by the rotating glass plate in the determination of the cross-section value. This is where the animated-beam technique comes into play, as will be explained in the next section.

III. ANIMATED CROSSED BEAMS

In most experiments with crossed-beam techniques, an absolute measurement of cross sections can be obtained only by assuming a certain profile for the beams. Laser-atom experiments usually assume a Gaussian spatial profile for the laser beam and a uniform profile for the atomic beam. The temporal profile of the laser pulses, if any, must also be included. While these assumptions are in general justified, they

might not be suitable for measuring absolute cross sections, for which every possible source of error must be tracked down and minimized in order to ensure the accuracy of the measurement.

One way to circumvent this problem is the so-called animated-crossed-beam technique, originally developed for electron-ion collisions by Brouillard and Defrance [24] and later adapted to laser-ion interaction (see Blangé *et al.* [26]). The underlying idea is simple: Instead of using two crossed *static* beams, one of the beams is *moved* across the other. The dependence of the cross section on the profiles of the two beams is then “erased” by integrating the signal over the beam displacement, leaving only integrated quantities to be measured. Let us first start from the ionization probability P , given by

$$P(y, z) = 1 - \exp \left[- \int \sigma \Phi(x, y, z) \frac{dx}{v} \right], \quad (1)$$

where v is the ions’ velocity and σ the detachment cross section and Φ denotes the local photon flux experienced at a position (x, y, z) within the reference axes defined in Fig. 1.

Let us consider the linear regime of photodetachment, i.e., reasonably low laser intensities, for which the exponential in the above equation can be expanded around the origin in terms of a power series. Keeping only the two first terms of the series yields a linear relation between the detachment probability and the cross section. The counting rate N of the detector is nothing but the detachment probability, averaged over the atomic beam section S and weighted by the detection efficiency η ,

$$N \simeq \sigma \eta \iint_S \frac{j(y, z)}{e} dy dz \int \Phi(x, y, z) \frac{dx}{v}, \quad (2)$$

where $j(y, z)$ is the local current density at a given position (y, z) on the ion beam section, and e is the elementary charge. This formula is valid for beams intersecting at right angles. The variable measured in the experiment is the counting rate $N(Y)$ as a function of the vertical displacement Y of the laser beam. Integration over Y yields

$$\begin{aligned} \int N(Y) dY &\simeq \frac{\sigma \eta}{e v} \iint_S j(y, z) dy dz \\ &\times \iint \Phi(x, y - Y, z) dx dY. \end{aligned} \quad (3)$$

The photon flux Φ is the ratio of the laser intensity to the photon energy $\hbar\omega$, hence the second integral on the right-hand side is nothing else than the laser power P_{laser} divided by $\hbar\omega$, which is independent of z . Thus only $j(y, z)$ depends on the spatial coordinates and its integration over the ion beam section is simply the ion current I_{H^-} . We obtain the following expression for the photodetachment cross section:

$$\sigma \simeq \frac{1}{\eta} \frac{\hbar\omega}{P_{\text{laser}}} \frac{e v}{I_{H^-}} \int N(Y) dY. \quad (4)$$

The sole assumption of a linear photodetachment regime, yielding the above formula, is much less stringent than that of a Gaussian laser beam and a uniform atomic beam. By integrating the signal, we were able to express the cross section in terms of a simple set of easily measurable quantities. This highlights the ease of implementation and robustness of the animated-crossed-beam method, which does not require the

laser and ion beam profiles to be fully characterized (e.g., M^2 factor, inhomogeneity).

In practice, the detachment rate is measured at different angles of the rotating plate (see Fig. 2). The vertical spacing ΔY corresponding to the angular increment has been measured by passing a razor blade, mounted on a high-accuracy translation stage, across the laser beam at a distance after the glass plate corresponding to the focus of the lens located right before it. By measuring the transmitted intensity as a function of the blade position, one can recover the vertical position of the beam center. The vertical increment is subsequently obtained by repeating the measurement at different angles of the plate. A straightforward application of the Snell-Descartes law of refraction gave a nearly identical ΔY , validating our measurement. Note that the variation of the refractive index of fused silica over the considered wavelength range is below 1%.

After converting the glass-plate angle into a vertical displacement, the integral on the right-hand side of Eq. (4) is easily computed with a Simpson numerical integration. As explained in the previous section, the power of the laser as well as the ion current are constantly monitored. From these values, the cross section can be immediately calculated.

IV. RESULTS

At each wavelength, the laser beam is scanned across the ion beam many times in order to secure good statistics. The resulting data, corrected for the laser power and the ion current, are shown in Fig. 4 for a laser wavelength of $\lambda = 850$ nm (1.4586 eV). On either side of the graph, the displacement of the laser beam is larger than the ion beam radius and the two beams do not overlap. Switching the laser on and off at large displacements did not change the neutrals counting rate of the CEM, thus ensuring that only the background counts are present. As the vertical displacement moves towards 0, there is an increasing overlap between both beams and the photodetachment signal rises on top of the background signal. The background is estimated by averaging three points at each extremity of the graph and then subtracted from the total counts

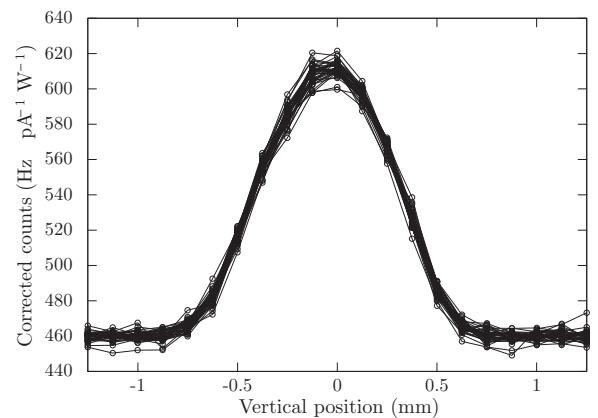


FIG. 4. Counting rate of the channel electron multiplier for different vertical displacements of the laser beam. The counts have been corrected for the H^- current and the laser power.

TABLE I. Present photodetachment cross sections (10^{-21} m^2) as a function of the photon energy (eV).

Photon energy (eV)	Wavelength (nm)	σ (10^{-21} m^2)	$\pm\Delta\sigma$ (10^{-21} m^2)
1.1654	1064	3.48	0.15
1.2398	1000	3.74	0.17
1.3051	950	3.82	0.17
1.3776	900	3.96	0.17
1.4586	850	3.96	0.17
1.5498	800	3.91	0.17
1.6531	750	3.90	0.17
1.7712	700	3.74	0.16

to obtain the net photodetachment signal, from which the cross section can be computed according to Eq. (4).

Figure 4 shows 40 scans of the vertical position at a wavelength of $\lambda = 850 \text{ nm}$ (1.4586 eV). For each, a value of the cross section is computed and the total cross section is the mean value, $3.96 \times 10^{-21} \text{ m}^2$. The standard deviation of the mean [27] is $0.02 \times 10^{-21} \text{ m}^2$, about 0.5% of the mean, highlighting the excellent repeatability of our measurements and providing the statistical error. Uncertainties arising from systematic effects are estimated as follows: the powermeter accuracy of 3% is given by the manufacturer; the vertical displacement of the laser beam is known with 2% precision, as estimated from the comparison of measured and calculated values; the 1% error on the current measurement is obtained by comparing the current measured by the two Faraday cups FC1 and FC2 and corresponds to the calibration accuracy of the electrometer; an uncertainty of 1% on the ions' velocity is given by the small variations of the source's acceleration voltage (4 kV); the uncertainty of 2% on the detection efficiency of the CEM has been previously established by Naji *et al.* [25]. Each of these values provide an upper limit a_+ and a lower limit a_- to the exact value a . As no further information is available about the probability distribution of a among the interval, we consider $[a_-, a_+]$ as a one-standard deviation confidence interval. The associated uncertainty is, consequently, following NIST's guidelines [27], $(a_+ - a_-)/2$ and the total error $\Delta\sigma$ is the quadrature sum of the various uncertainties. The above procedure was repeated by steps of 50 nm in the 700- to 1000-nm range, with an additional measurement at 1064 nm, yielding the results presented in Table I and compared to the existing data in Figs. 5 and 6 (circles).

As shown in Fig. 5, the present measurement agrees well with the absolute measurement of Popp and Kruse [19]. These authors used the spectrum of a well-characterized hydrogen-arc lamp and, by modeling the partial local thermal equilibrium within the arc, could infer absolute values for the photodetachment cross section. The wavelength dependence of our measured cross section matches the relative measurement of Smith and Burch [18], which is put on an absolute scale for comparison, using one of the most robust theoretical data available, namely that of Venuti and Decleva [10]. Smith and Burch performed the measurement of the photodetachment cross section of the D^- ion within a crossed-beam configuration. The

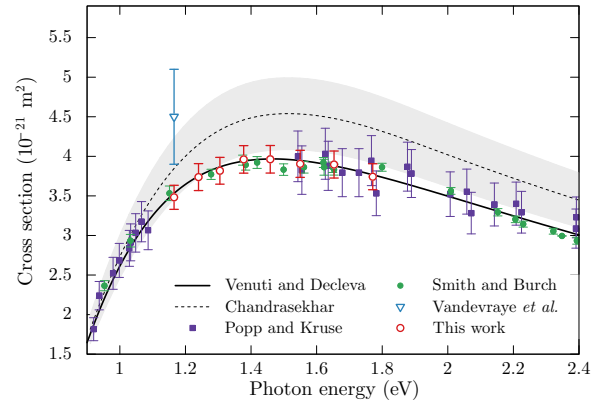


FIG. 5. (Color online) Experimental photodetachment cross section (10^{-21} m^2) as a function of the photon energy (eV). The empty circles and triangles are, respectively, the present work and the work of Vandevraye *et al.* [22]. The full squares are from Popp and Kruse [19] and the disks are the relative measurement of Smith and Burch [18] set on an absolute scale using the calculation of Venuti and Decleva [10] (shown by the full line). The wavelength integrated measurements of Branscomb and Smith [17] lie within $\pm 10\%$ of the calculation of Chandrasekhar [3] multiplied by 1.01 (dashed line), as depicted by the shaded area.

light source was a carbon projection arc lamp combined with narrow band filters, providing quasimonochromatic intense light. The measurement of the free electron current, the ion current, and the light power yielded a relative value for the cross section. These two methods differ from the present experiment, and the good agreement both in shape and magnitude therefore gives confidence in the validity of the values obtained.

A measurement of the photodetachment cross section has been recently performed by Vandevraye *et al.* [22] with a pulsed Nd:YAG laser and is also shown in Fig. 5. The cross

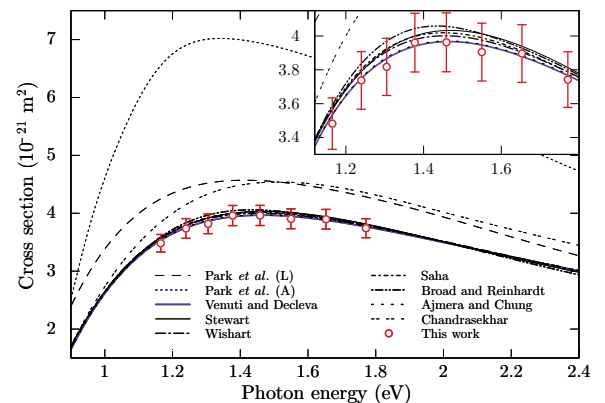


FIG. 6. (Color online) Photodetachment cross section (10^{-21} m^2) as a function of the photon energy (eV). The empty circles are the present work. The curves are theoretical values from Park *et al.* [15] in the length (dashed) and acceleration (densely dotted) gauges, Venuti and Decleva [10] (full thick), Stewart [5] (full thin), Wishart [6] (long dash-dotted), Saha [7] (dash-dotted), Broad and Reinhardt [8] (dash-doubly dotted), Ajmera and Chung [9] (dotted), and Chandrasekhar [3] (doubly dotted).

section was measured by means of several saturation-based techniques, thus avoiding the approximation of the linear regime. To obtain the cross section, the spatial and temporal profiles of the photon flux had to be assumed Gaussian while the ion density was assumed uniform. Although justified, these assumptions are not exact and may therefore introduce discrepancies. This measurement lies at the higher limit of compatibility with the results of Popp and Kruse [19] compiled in their table. Note that the value of $3.6(3) \times 10^{-21} \text{ m}^2$ quoted in Ref. [22] was obtained from the crossed beam values of Smith and Burch [18] scaled by Popp and Kruse [19].

For the sake of completeness, one must mention the first absolute measurement made by Branscomb and Smith [17] in the mid-1950s. They measured the integrated cross section of the photodetachment of H^- by illuminating the anion beam at right angle with a tungsten lamp combined with a set of sharp cutoff filters. The cross section being integrated over a wide range of photon energies, no direct comparison can be made. The authors, however, computed the ratio of their cross section to the values obtained by Chandrasekhar [3], obtaining an average of 1.01 ± 0.10 . Therefore, the cross section computed by Chandrasekhar, multiplied by 1.01, is plotted in Fig. 5 along with a shaded area defining a 10% interval around the theoretical curve. It appears to be fully compatible with the measurements of Popp and Kruse [19] and Vandevraye *et al.* [22].

The absolute photodetachment cross section was also investigated by Bacal and Hamilton [20] and Nishiura *et al.* [21] by means of lasers in an attempt to monitor the production of H^- and D^- ions within fusion plasmas. The fraction of photodetached ions as a function of the laser pulse energy was measured, and a subsequent fit with the theoretical photodetachment probability, depending on the cross section, ensured the validity of the method. However, the important spread of the data points allows to confirm only the order of magnitude of the cross section.

As shown in Fig. 6, the agreement of the present measurement with most theoretical results is excellent over the whole wavelength range covered by the experiment, particularly with that of Ajmera and Chung [9] and of Venuti and Decleva [10]. The latter is a state-of-the-art calculation which was internally validated by the perfect matching of the cross-section values obtained within the different gauges (length, velocity, and acceleration), and its accuracy is estimated to be better than $0.001 \times 10^{-21} \text{ m}^2$. The value computed at 1064 nm (1.1653 eV) is $\sigma = 3.52 \times 10^{-21} \text{ m}^2$ and agrees within error bars with the present value $\sigma = 3.48(15) \times 10^{-21} \text{ m}^2$. The value of Vandevraye *et al.* [22] is $\sigma = 4.5(6) \times 10^{-21} \text{ m}^2$ and lies 1.5σ above that of Venuti and Decleva.

A few theoretical values depart from the commonly obtained cross section. In particular, the adiabatic approximation in hyperspherical coordinates, adopted both by Fink and Zoller [16] and Park *et al.* [15], led to the significantly higher results shown in Fig. 6. Park *et al.* gave a detailed account of the possible causes of the discrepancy, accounting for the lower reliability of the adiabatic hyperspherical approximation in the regions of the configuration space where the gauges used have the largest weight. It also applies to Fink and Zoller's calculation, who obtained results identical to Park *et al.* within numerical accuracy. The adiabatic hyperspherical approach was later extended from single-channel to coupled-channels calculations by, e.g., Masili and Starace [12]. Including no more than four channels, their computed photodetachment cross section converged to the values of Stewart [5], which lie in the range of most theoretical works. The early work of Chandrasekhar [3] also departs from the commonly obtained values. This pioneering calculation was performed with a model potential without explicitly taking into account electron correlations.

V. CONCLUSION

We reported an experimental determination of the photodetachment cross section of H^- in the 700- to 1064-nm wavelength range. The animated-crossed-beam method was adapted to the laser-atom case and provided a direct relation between the cross section and easily measurable quantities: laser power, ion current, and integrated detachment signal. The results obtained with this method were found to be in excellent agreement with most of the previous experimental determinations and with recent, compelling theoretical studies.

The general method of the animated crossed beams is versatile and can be easily applied to other one photon processes. The wavelength range of the present study could be extended by use of another laser. The photodetachment cross section of other negative ions could also be measured with a similar setup, e.g., He^- for which we performed preliminary measurements [28]. Further extension of the animated-beam method to the pulsed laser case will be the subject of a forthcoming publication.

ACKNOWLEDGMENTS

The authors thank H. Bachau, C. Blondel, and B. Piraux for fruitful discussions. This work was supported by the Fonds de la Recherche Scientifique - FNRS through IISN Contract No. 4.4504.10.

-
- [1] A. R. P. Rau, *J. Astrophys. Astron.* **17**, 113 (1996).
 - [2] D. R. Bates and H. S. W. Massey, *Mon. Not. R. Astron. Soc.* **106**, 432 (1946).
 - [3] S. Chandrasekhar, *Astrophys. J.* **102**, 395 (1945).
 - [4] A. G. Abrashkevich and M. Shapiro, *Phys. Rev. A* **50**, 1205 (1994).
 - [5] A. L. Stewart, *J. Phys. B* **11**, 3851 (1978).

- [6] A. W. Wishart, *Mon. Not. R. Astron. Soc.* **187**, 59P (1979).
- [7] H. P. Saha, *Phys. Rev. A* **38**, 4546 (1988).
- [8] J. T. Broad and W. P. Reinhardt, *Phys. Rev. A* **14**, 2159 (1976).
- [9] M. P. Ajmera and K. T. Chung, *Phys. Rev. A* **12**, 475 (1975).
- [10] M. Venuti and P. Decleva, *J. Phys. B* **30**, 4839 (1997).
- [11] A. S. Kheifets and I. Bray, *Phys. Rev. A* **58**, 4501 (1998).
- [12] M. Masili and A. F. Starace, *Phys. Rev. A* **62**, 033403 (2000).

- [13] A. M. Frolov, *J. Phys. B* **37**, 853 (2004).
- [14] T. N. Chang and X. Tang, *Phys. Rev. A* **44**, 232 (1991).
- [15] C.-H. Park, A. F. Starace, J. Tan, and C.-D. Lin, *Phys. Rev. A* **33**, 1000 (1986).
- [16] M. G. J. Fink and P. Zoller, *J. Phys. B* **18**, L373 (1985).
- [17] L. M. Branscomb and S. J. Smith, *Phys. Rev.* **98**, 1028 (1955).
- [18] S. J. Smith and D. S. Burch, *Phys. Rev.* **116**, 1125 (1959).
- [19] H.-P. Popp and S. Kruse, *J. Quant. Spectrosc. Radiat. Transf.* **16**, 683 (1976).
- [20] M. Bacal and G. W. Hamilton, *Phys. Rev. Lett.* **42**, 1538 (1979).
- [21] M. Nishiura, M. Sasao, and M. Bacal, *J. Appl. Phys.* **83**, 2944 (1998).
- [22] M. Vandevraye, P. Babilotte, C. Drag, and C. Blondel, *Phys. Rev. A* **90**, 013411 (2014).
- [23] M. Dörr, J. Purvis, M. Terao-Dunseath, P. G. Burke, C. J. Joachain, and C. J. Noble, *J. Phys. B* **28**, 4481 (1995).
- [24] P. Defrance, F. Brouillard, W. Claeys, and G. V. Wassenhove, *J. Phys. B* **14**, 103 (1981); F. Brouillard and P. Defrance, *Phys. Scr.* **T3**, 68 (1983).
- [25] A. Naji, K. Olamba, J. P. Chenu, S. Szücs, M. Chibisov, and F. Brouillard, *J. Phys. B* **31**, 2961 (1998).
- [26] J. J. Blangé, X. Urbain, H. Rudolph, H. A. Dijkerman, H. C. W. Beijerinck, and H. G. M. Heideman, *J. Phys. B* **29**, 2763 (1996).
- [27] B. N. Taylor and C. N. Kuyatt, NIST Technical Note 1297, 1994 Edition (U.S. Government Printing Office, Washington, DC, 1994).
- [28] M. S. Brouri, P. J. M. van der Burgt, J. Jureta, and X. Urbain, in *XXIII ICPEAC, Abstracts of Contributed Papers*, edited by J. Anton, H. Cederquist, M. Larsson, E. Lindroth, S. Mannervik, H. Schmidt, and R. Schuch (Stockholm University, Stockholm, 2003), p. We021.